

See discussions, stats, and author profiles for this publication at: <https://www.researchgate.net/publication/51074042>

# Physicochemical Properties of Methylcellulose and Dodecyltrimethylammonium Bromide in Aqueous Medium

ARTICLE in THE JOURNAL OF PHYSICAL CHEMISTRY B · MAY 2011

Impact Factor: 3.3 · DOI: 10.1021/jp110247r · Source: PubMed

CITATIONS

14

READS

32

7 AUTHORS, INCLUDING:



**Clara I. D. Bica**

Universidade Federal do Rio Grande do Sul

30 PUBLICATIONS 268 CITATIONS

SEE PROFILE



**Irene T S Garcia**

Universidade Federal do Rio Grande do Sul

40 PUBLICATIONS 202 CITATIONS

SEE PROFILE



**Fabiano Pereira**

Federal University of Minas Gerais

45 PUBLICATIONS 413 CITATIONS

SEE PROFILE



**Cristiano Giacomelli**

Universidade Federal de Santa Maria

73 PUBLICATIONS 1,331 CITATIONS

SEE PROFILE

# Physicochemical Properties of Methylcellulose and Dodecyltrimethylammonium Bromide in Aqueous Medium

Marcos A. Villetti,<sup>\*,‡</sup> Clara I. D. Bica,<sup>§</sup> Irene T. S. Garcia,<sup>§</sup> Fabiano V. Pereira,<sup>†</sup> Francieli I. Ziembowicz,<sup>‡</sup> Carmen L. Kloster,<sup>‡</sup> and Cristiano Giacomelli<sup>‡</sup>

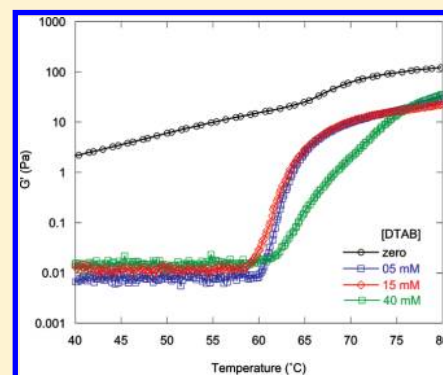
<sup>‡</sup>Departamento de Física, Centro de Ciências Naturais e Exatas, Universidade Federal de Santa Maria, 97105-900 Santa Maria-RS, Brazil

<sup>§</sup>Instituto de Química, Universidade Federal do Rio Grande do Sul, 91501-970 Porto Alegre-RS, Brazil

<sup>†</sup>Departamento de Química, Universidade Federal de Minas Gerais, 31270-901 Belo Horizonte-MG, Brazil

<sup>‡</sup>Departamento de Química, Centro de Ciências Naturais e Exatas, Universidade Federal de Santa Maria, 97105-900 Santa Maria-RS, Brazil

**ABSTRACT:** Interactions between uncharged polymers and cationic surfactants are considered weaker than interactions with the anionic analogues. This work describes the binding occurring between methylcellulose (MC) and the cationic surfactant DTAB in aqueous medium. In the absence of salt, MC–DTAB exhibits a maximum in hydrodynamic radius,  $R_{h,slow}$ , with the increase in the surfactant concentration. Otherwise, in presence of salt the MC–DTAB system shows only a linear increase of  $R_{h,slow}$ . CAC is lower than the CMC, which is taken as an evidence of binding between the cationic surfactant and neutral polymer that induces the aggregation process. Static light scattering, rheology and micro-DSC results highlight the hydrophobic MC–DTAB association. Salt-out and the salt-in effects were observed in presence of DTAB, with a clear transition at concentration values close to the CMC, as judged from rheological and micro DSC measurements. Indeed, DTAB affects both the pattern of the sol–gel transition and the gel strength.



## INTRODUCTION

Interactions involving nonionic polymers and ionic surfactants in aqueous solutions have generated considerable interest in the research community because their physicochemical properties are very important in many industrial applications (pharmaceutical formulations, cosmetics products, food additives, enhanced oil recovery, paints and coating products etc.).<sup>1–11</sup> The amphiphilic nature of surfactants grants them special properties to introduce interactions with water-soluble polymer, especially those with hydrophobic segments.<sup>12</sup> Methylcellulose is a hydrophobically modified nonionic water-soluble polysaccharide produced by the methylation of native cellulose. MC has been used, for example, in pharmaceutical industry to produce polymeric films that can act as protective layers for tablets and rate controlling barriers to drug release.<sup>13</sup>

Cationic surfactants such as *n*-alkyltrimethylammonium bromide homologues (RTAB, with R equal to C<sub>16</sub>, C<sub>14</sub>, and C<sub>12</sub>) are important pharmaceutically because of their bactericidal activity against a wide range of gram-positive and some gram-negative organisms.<sup>13</sup> In addition, aqueous MC solutions exhibit an phenomenon of gelling upon heating in contrast to natural polymers such as gelatin, agarose or carrageenan that gel upon cooling.<sup>14,15</sup> Several factors, such as pH, presence of salts, type and concentration of surfactants, and so forth, can alter the sol–gel transition of MC. It was observed that the surfactant molecules have a tendency to aggregate around such hydrophobic segments of the polymer chains in aqueous solution, inducing changes in the thermal

behavior of cellulose derivatives during the gelation process.<sup>12,16,17</sup> It is established that polymer–surfactant interaction can be described by two critical concentrations in a system of fixed polymer concentration and increasing amounts of surfactant. The first represents the concentration at which surfactant molecules start to bind to the polymer chain and is known as critical aggregation concentration (CAC). Since CAC is, in general, lower than the CMC of the surfactant, this means that the polymer–surfactant complex is energetically more stable than surfactant molecules in regular micelles. The second critical concentration occurs when the sites on polymer are saturated with surfactant molecules and this point is called polymer saturation point (PSP).<sup>18,19</sup> These critical concentrations can be determined through different techniques such as electrical conductivity,<sup>20–23</sup> viscosity,<sup>11</sup> microcalorimetry,<sup>24</sup> tensiometry,<sup>22,23,25,26</sup> and steady-state fluorescence.<sup>25,27–31</sup>

The interaction of cellulose ethers with cationic surfactants compared with anionic ones has been found to be considerably weak.<sup>32,33</sup> A few works describing the interaction of MC with hexadecyltrimethylammonium bromide (CTAB) surfactant with a longer alkyl chain, have been published.<sup>18,34,35</sup> Li et al.<sup>35</sup> recently reported the effect of surfactant type on sol–gel transition of MC as studied by micro-DSC and rheology. The authors found that both CTAB and sodium dodecyl sulfate (SDS) impart salt-out and salt-in

**Received:** October 26, 2010

**Revised:** March 24, 2011

**Published:** April 25, 2011

effects to the sol–gel transition of MC depending on their concentration. For both surfactants, there is a critical value below and above which a salt-out and a salt-in effect appear, respectively. This critical value was close to the CMC of the cationic surfactant, and close to the CAC of the anionic one. Although CTAB has a much smaller CMC than SDS, the salt-out effect of CTAB is much weaker than SDS. CTAB acts as a strong salt-in agent for MC rather than a salt-out one. Dar et al.<sup>36</sup> studied the effect of sodium chloride and hydrophobic salts (sodium benzoate, sodium hexanoate) on CAC, gelation temperature, and viscosity of the MC–CTAB system employing rheological and steady state fluorescence measurements. It was observed that the gelation temperature of the MC–DTAB system, with surfactant concentration above CAC, presents a huge decrease in the presence of NaCl and a small one with the hydrophobic salt. This behavior was rationalized by taking into account the salt type. NaCl decreases water content adjacent to alkyl group of the MC, and thus a lower temperature is needed to destroy the surfactant cage structure on the hydrophobic groups of the MC. In the case of hydrophobic salts there are two opposite effects occurring on the gelation temperature: (i) due to its particular solubilization characteristics, the hydrophobic salt promotes an enhancement of the interaction between CTAB and MC and then contributes to an increase in the gelation temperature; (ii) the hydrophobic salt reduces the solvent polarity and then causes a decrease in the gelation temperature. However, the overall effect of the hydrophobic salt is a small decrease in the gelation temperature in contrast to NaCl.

It is currently well-known that several properties in cellulose ethers—alkyltrimethylammonium bromide homologue systems such as cloud point and viscosity depend on surfactant chain length. That is, the interaction is affected by surfactant hydrophobicity.<sup>32,37,38</sup> Sardar et al.<sup>38</sup> recently reported that a surfactant with a long alkyl chain (CTAB) changes the cloud point of HPMC much more than a short alkyl chain (DTAB). To the best of our knowledge, there are no reports on the effect of a cationic surfactant with a relatively short alkyl chain such as dodecyltrimethylammonium bromide on the solution and gelation properties of MC.

The interaction between a nonionic polymer with a cationic surfactant in aqueous solutions may produce distinct patterns of the sol–gel transition, as well as affect the gel strength. In the present paper, different physicochemical properties on the interaction polymer–surfactant are discussed at different MC (dilute regime and gel phase) and DTAB concentrations (below and above its CMC). Dynamic light scattering results are presented on the conformation and hydrodynamical behavior of MC polymer chain as a function of DTAB surfactant in salt free and, for comparison, in the presence of salt (NaCl). The electrical conductivity and steady-state fluorescence measurements are used to determine the onset for the formation of polymer–surfactant aggregation complex. The effect of the DTAB on the MC gel transition temperature is investigated through static light scattering, rheology and micro-DSC. This study on the interaction between MC–DTABs may contribute to better understand the nature and strength of intermolecular forces between a nonionic polymer and amphiphilic substances used in several industrial applications.

## ■ EXPERIMENTAL SECTION

**Materials.** Methylcellulose (SM-4000) was provided by the Shin-Etsu company (Tokyo, Japan). The degree of methoxyl substitution (DS) specified by the manufacturer was 1.8. Dodecyltrimethylammonium bromide (DTAB, 98%) and NaCl (99.5%) were purchased

from Fluka and Sigma-Aldrich, respectively. The materials were used as received without further purification. Pure water was collected from a Millipore apparatus Alpha Q (conductivity less than  $0.05 \mu\text{S cm}^{-1}$ ) and used to prepare the solutions. The pyrene (98%) probe was purchased from Aldrich and was recrystallized twice from ethanol solution.

Solutions of MC were prepared by a standard technique.<sup>39</sup> A weighed amount of MC was mixed with approximately 50 % of the total amount of water at 70 °C. This solution was shaken at this temperature for 2 h. Water at 5 °C was then added to the system, and the mixture was stirred at 5 °C for about 12 h in order to obtain a transparent and homogeneous solution. The resulting solution was dialyzed against Milli-Q water during 7 days by using cellulose membrane (Viskase, cutoff  $1.2 \times 10^4 - 1.6 \times 10^4 \text{ g mol}^{-1}$ ). After dialysis, the stock solution was passed through 8.00 and  $0.45 \mu\text{m}$  membrane filters (Millipore), consecutively. Finally, the MC concentration was determined by drying a known volume of the solution to constant weight at 105 °C. This method is suitable for determination of cellulose derivative concentration since these polymers lose their water of hydration and precipitate out of solution upon heating. After dialysis, MC presents weight-averaged molecular weight  $M_w = 3.6 \times 10^5 \text{ g mol}^{-1}$ , radius of gyration  $R_g = 68.7 \text{ nm}$  and second virial coefficient  $A_2 = 4.94 \times 10^{-4} \text{ mol cm}^3 \text{ g}^{-2}$  (values obtained in 100 mM NaCl at 298 K through static light scattering by using Zimm plot extrapolation procedure). Polymer solutions at various concentrations were prepared by diluting stock solution of MC and, when necessary, the stock solution of surfactant (DTAB) and salt (NaCl) was added to obtain the desired contents. The interaction polymer–surfactant was examined at different surfactant concentrations below and above the CMC. All MC–DTAB samples were stirred for 12 h at room temperature before the measurements. In order to remove dust for the light scattering experiments, the solutions were filtered through  $0.45 \mu\text{m}$  membrane filters (Millipore) and centrifuged at 4000 rpm for 90 min. Pyrene was used as probe to obtain the fluorescence spectra. The probe solution was prepared by evaporating the suitable volume of acetone stock solution (pyrene  $1 \times 10^{-7} \text{ mol L}^{-1}$ ), followed by dissolution of the remaining solid in the MC–surfactant solution. The flasks were recovered with aluminum paper to avoid contact with light. All MC–DTAB solutions were stirred overnight at room temperature to allow the resolubilization of the probe before fluorescence measurements.

**Methods. Electrical Conductivity.** Electrical conductivity was measured by using an Oakton Con 100 series conductivity meter. The solutions were thermostated at  $25.0 \pm 0.1 \text{ °C}$  with a water bath for at least 10 min before the readings were taken. Slopes of linear regions of the conductivity versus surfactant concentration plot were obtained by use of linear regression routine. The CAC and CMC values for the MC–DTAB and DTAB systems, respectively, were determined from the intersection points of these lines. The polymer concentration was maintained constant at  $1 \text{ g L}^{-1}$  a value quite below the coil overlap concentration  $C^* = 5.6 \text{ g L}^{-1}$  calculated from  $C^* = (A_2 M_w)^{-1}$ .

**Fluorescence.** The steady-state fluorescence measurements were obtained on a Cary Eclipse (Varian) in the corrected mode with excitation wavelength of 336 nm and 2.5 mm slit in the range 350–500 nm with cell holder thermostated by a circulating ethylene glycol bath at  $25 \pm 0.4 \text{ °C}$ . It is known that the ratio  $I_1/I_3$ , taken from first (372 nm) and third (384 nm) vibronic peaks in the pyrene emission spectrum, shows linear dependence

with the local micropolarity in organized systems.<sup>40</sup> The pyrene concentration was kept as low as  $10^{-7}$  mol L<sup>-1</sup> to avoid the excimer formation, which may occur when the concentration is higher than  $10^{-4}$  mol L<sup>-1</sup>. The interaction polymer–surfactant was determined at a fixed polymer ( $1\text{ g L}^{-1}$ ) and salt concentrations ( $100\text{ mmol L}^{-1}$ ) at different surfactant contents.

**Light Scattering.** Static (SLS) and dynamic (DLS) light scattering measurements were made on a Brookhaven Instruments goniometer, with He–Ne laser Spectra Physics at 632.8 nm. For DLS measurements, a 264-Channel BI-9000 AT correlator covering seven decades in delay time was used. The samples were thermostated in a refractive-index-matching liquid (decalin). In the dynamic light scattering (DLS) experiments, the full homodyne autocorrelation function  $G^2(\tau)$  of the scattered intensity was measured:

$$G^2(\tau) = \langle I(0)I(\tau) \rangle \quad (3)$$

and normalized by dividing it by the average intensity squared  $\langle I \rangle^2$ . The normalized intensity time autocorrelation function,  $g^{(2)}(\tau)$ , is related to the normalized electric field autocorrelation function,  $g^{(1)}(\tau)$ , by the Siegert relation<sup>41</sup>

$$g^{(2)}(\tau) = 1 + \beta |g^{(1)}(\tau)|^2 \quad (4)$$

where  $\beta$  is the spatial coherence factor. In order to characterize the hydrodynamic behavior of the polymer–surfactant complex solutions,  $g^{(1)}(\tau)$  was expressed by a continuous distribution of decays:

$$g^{(1)}(\tau) = \int A(\Gamma) e^{(-\Gamma\tau)} d\Gamma \quad (5)$$

where  $A(\Gamma)$  is the amplitude of the relaxation modes and  $\Gamma$  is the relaxation frequency of the modes. The  $g^{(1)}(\tau)$  was analyzed by means of constrained regularization (CONTIN) method developed by Provencher<sup>42,43</sup> to obtain the distribution of decay times and their corresponding amplitudes. The translational diffusion coefficient was calculated from

$$D = \frac{\Gamma}{q^2} \quad (6)$$

The apparent hydrodynamic radius,  $R_h$ , was obtained from the apparent diffusion coefficient at the fixed polymer concentration of MC ( $1\text{ g L}^{-1}$ ) and scattering angle  $\theta = 90^\circ$  according to the Stokes–Einstein relation:

$$D = \frac{k_B T}{f} \quad (7)$$

Here,  $k_B T$  is the Boltzmann energy,  $f = 6\pi\eta R_h$  is the friction coefficient, and  $\eta$  is the solvent viscosity. The DLS experiments took place at  $25^\circ\text{C}$ , whereas the SLS experiments were carried out in a temperature range from  $20$  to  $80^\circ\text{C}$  in order to characterize the surfactant effect on the gelation of the polymer. For the SLS experiments, the light scattered was measured at  $90^\circ$  of scattering angle. The solutions were thermostated for 10 min at each temperature before the data acquisition.

**Rheological Measurements.** Rheological experiments were carried out on a stress-controlled rheometer (TA Instruments AR-G2). A cone–plate geometry with a cone diameter of 60 mm and an angle of  $2^\circ$  (truncation =  $52\text{ }\mu\text{m}$ ) was used, and temperature was controlled by a Peltier plate. The polymer solution was loaded onto the plate equilibrated at  $10^\circ\text{C}$ . The gap was then closed using exponential sample compression mode to avoid shear effects. Excess

of sample was trimmed using flat-ended tool while the bearing was locked to prevent rotation. A solvent trap system filled with water was used to minimize evaporation in all experiments. Dynamic viscoelastic properties (shear storage modulus  $G'$  and loss modulus  $G''$ ) were measured by oscillatory shear experiments performed at a fixed frequency of 1 Hz during a temperature ramp from  $10$  to  $80^\circ\text{C}$  at a heating rate of  $1^\circ\text{C min}^{-1}$  (similar to that used in the micro-DSC measurements). A gap match temperature compensation coefficient of  $0.6\text{ }\mu\text{m }^\circ\text{C}^{-1}$  was applied. A strain amplitude of 3% was applied in all dynamic tests to ensure that the deformation was within the linear viscoelastic regime for both sol and gel states. The linear viscoelastic region was determined by a strain sweep from 0.001 to 15% performed at frequency of 1 Hz at  $25^\circ\text{C}$  (sol state) and  $75^\circ\text{C}$  (gel state). The sol–gel transition temperature was determined from the onset of the abrupt increase of dynamic storage modulus  $G'$ , as suggested by Li et al.<sup>44</sup>

**Microthermal Analysis.** Calorimetric measurements were carried out on a micro differential scanning calorimetric (VP-DSC high-sensitivity, Microcal Inc., MA). Every test included heating the sample from  $25$  to  $80^\circ\text{C}$  and then cooling it back to  $25^\circ\text{C}$  at a rate of  $1^\circ\text{C min}^{-1}$ . The samples were heated and cooled twice to examine the thermoreversibility of the gelation process. The sample cell had a volume of 0.5 mL. Samples were kept at  $25^\circ\text{C}$  for 20 min before the scan was started. Reference thermograms were recorded under the same conditions by filling both sample and the reference cells with water. The gelation temperature was determined from the peak temperature of the endothermic curve of the second heating.

## RESULTS AND DISCUSSION

**A. MC–DTAB in Diluted Regime.** First, the polymer–surfactant interaction was studied in the diluted regime ( $C < C^*$ ) in order to determine, independently, the characteristic parameters of methylcellulose and DTAB in solution. Then, the surfactant effect on sol–gel transition temperature of MC at polymer concentration close to  $C^*$  was analyzed since it is well-known that MC forms a gel above  $3\text{ g L}^{-1}$ .<sup>44</sup>

Electrical conductivity is a convenient method to investigate the interaction between a non ionic polymer and an ionic surfactant. The conductometry profiles of DTAB–water and MC–DTAB versus surfactant concentration at MC  $1\text{ g L}^{-1}$  in the absence of salt are shown in Figure 1. Initially, the conductivity of the DTAB–water increased linearly with concentration. The curve presents a distinct inflection point close to  $15\text{ mmol L}^{-1}$  and beyond this point the conductivity increases linearly with a lower slope. This value is the CMC of the surfactant and agrees very well with the values found in the literature for DTAB.<sup>11,45,46</sup> For the system MC–DTAB, the inflection change of the conductivity curve occurs close to  $8.5\text{ mmol L}^{-1}$  and indicates the CAC value. As expected, the CAC value is lower than the CMC indicating that the association of DTAB to MC is thermodynamically favored and it is taken as evidence of binding of the surfactant to the polymer. This behavior may be understood as a decrease of the electrostatic headgroup repulsion of the shell of the micelle due to the reduction of the surface charge density because of the presence of polymer.<sup>28</sup> Generally the degree to which the CAC is lower than CMC depends on the magnitude of the interaction polymer–surfactant. Several works have evidenced the interaction between a water-soluble neutral polymer and an anionic surfactant,



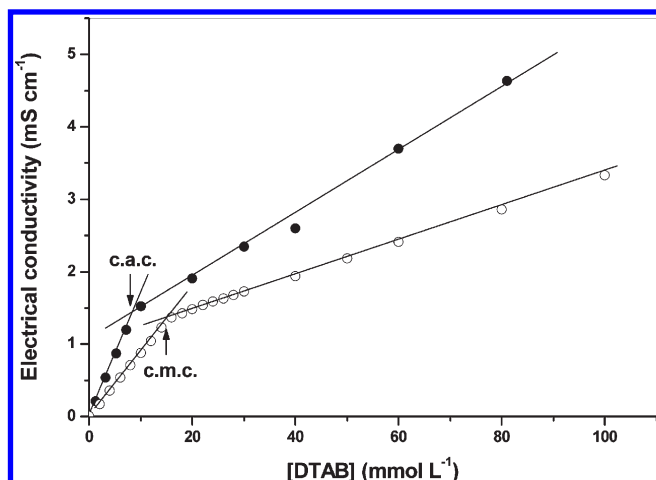


**Figure 1.** Electrical conductivity of solutions at 25 °C without salt: (○) DTAB and (●) methylcellulose/DTAB system.

**Table 1.** Thermodynamic Parameters at 298 K

	CMC or CAC (mmol L <sup>-1</sup> )	$\beta$	$\Delta G_m^\circ$ (kJ mol <sup>-1</sup> )
DTAB–water	15.0	0.74	–35.4
MC–DTAB	8.5	0.71	–37.1

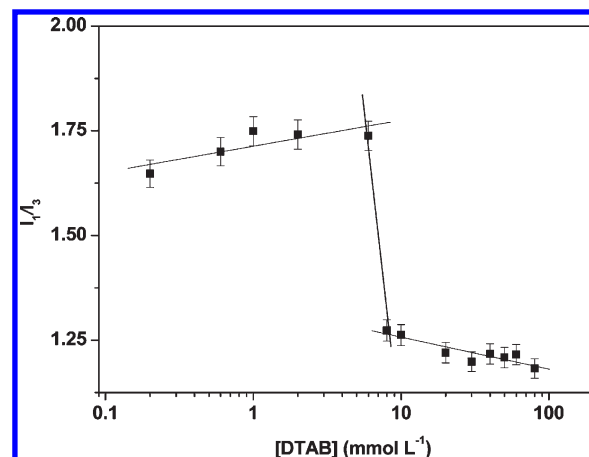
contrary to the case of cationic surfactant whose interaction has been considered weak.<sup>32,33</sup> This fact has been explained considering the physicochemical behavior of charged species in solution: (a) the higher bulkiness of cationic headgroup, due to hydration, as compared to anionic surfactant, promotes the decrease of the interaction with the nonionic polymer;<sup>47</sup> (b) the hydration shell of the uncharged polymer favors the interaction with the anionic surfactant.<sup>48</sup> However, there are evidences of a complex formation between cellulose derivatives and *n*-alkyltrimethylammonium bromide series.<sup>20,49</sup> When two types of interactions are possible simultaneously, a general rule determining the priority for an ionic surfactant to bind to neutral polymer was verified to be hydrophobic interaction > ion–dipole interaction.<sup>18</sup> Furthermore, the association of ionic surfactant with neutral polymer is a cooperative phenomenon and viewed as a polymer-induced micellization.

Table 1 shows the most important thermodynamic parameter of aggregation called standard Gibbs free-energy of micellization ( $\Delta G_m^\circ$ ), the critical concentrations, as well as the degree of counterion binding ( $\beta$ ) for the DTAB–water and MC–DTAB systems calculated using the mass action model for micelle formation of ionic surfactant.<sup>50</sup> The following relations were used for the calculations<sup>51,52</sup>

$$\beta = 1 - \frac{S_2}{S_1} \quad (8)$$

$$\Delta G_m^\circ = (1 + \beta)RT \ln X_{CMC} \quad (9)$$

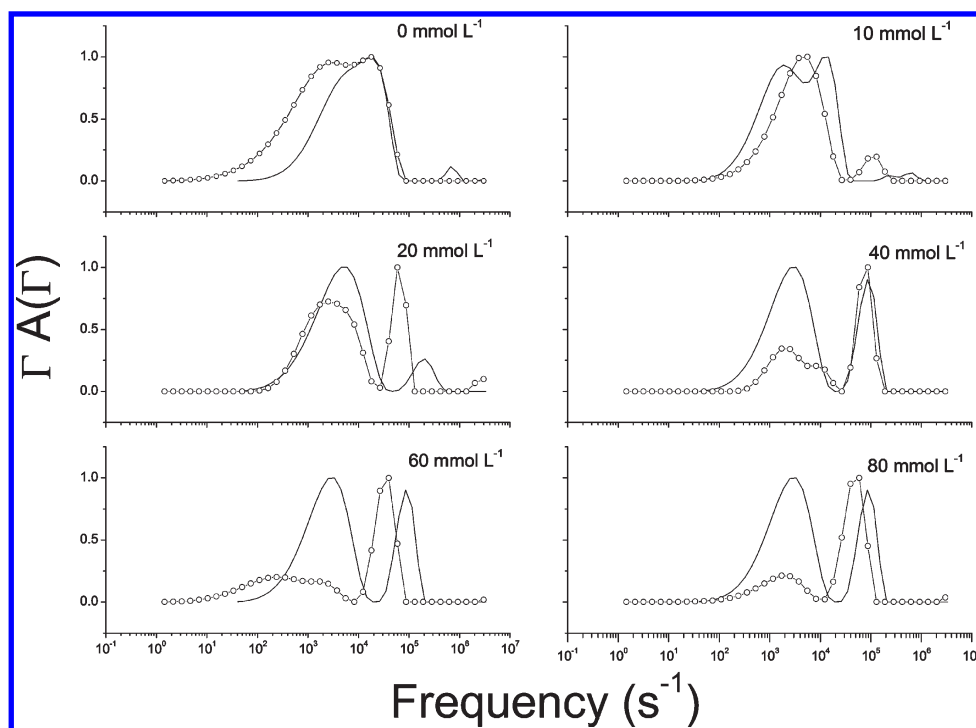
where  $S_2/S_1$  is the ratio of the slopes above and below the CMC,  $R$  is the universal gas constant,  $T$  is the absolute temperature and  $X_{CMC}$  is the mole fraction of surfactant molecules at the CMC. Concerning the degree of counterion binding, if we compare the  $\beta$  values between DTAB–water and MC–DTAB systems, we



**Figure 2.** Dependence of the  $I_1/I_3$  ratio on surfactant concentration in aqueous solution of 1 g L<sup>-1</sup> methylcellulose.

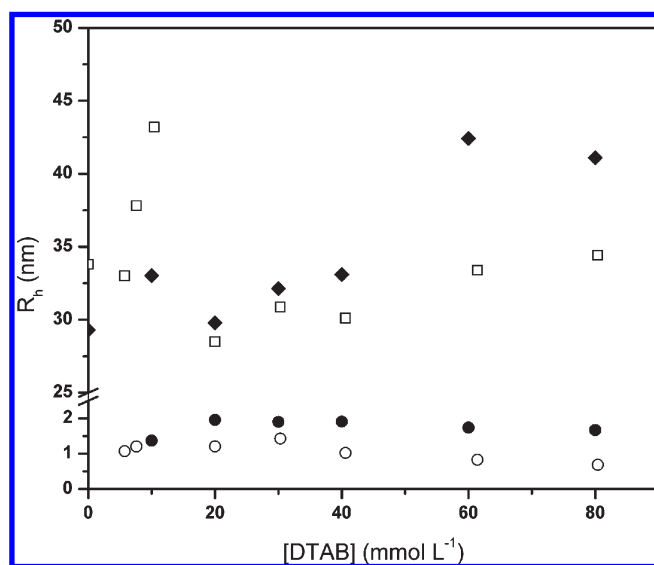
verified that this parameter decreased in the presence of the MC. The DTAB and MC–DTAB have 74 and 71% binding of Br<sup>-</sup> ions with the micelles, respectively. The decrease of  $\beta$  is a consequence of a decrease in the charge density due to a reduction in the aggregation number of DTAB micelles induced by the presence of the natural polymer. Moreover, taking into account the thermodynamic result we verified that micellization is a spontaneous process. The presence of MC tends to diminish even more the standard Gibbs free-energy, denoting its influence on stabilizing the DTAB micelles. A lower  $\Delta G_m^\circ$  to MC–DTAB when compared to DTAB–water and a lower value of CAC than CMC demonstrate that the MC polymer induces the aggregation process. It is important to note that the enthalpic ( $\Delta H_m^\circ$ ) and entropic ( $T\Delta S_m^\circ$ ) contribution play an important role in the micellization.

We also determined the CAC through the use of a probe molecule, i.e. pyrene, which presents different fluorescence behavior in different environments. The ratio  $I_1/I_3$  of the intensities of the first (372 nm) and third (384 nm) vibronic peak of monomeric pyrene, shows linear dependence with the local micropolarity. Pyrene was chosen as probe also because of the high emission efficiency and hydrophobicity. The emission band  $I_1$  is more intense than the  $I_3$  in polar environment and  $I_1/I_3$  shows typical values around 1.9. Otherwise,  $I_1/I_3$  changes to around 0.6 when pyrene is in contact with apolar media. Figure 2 shows the ratio  $I_1/I_3$  from pyrene fluorescence as a function of surfactant concentration at MC 1 g L<sup>-1</sup> in the presence of 100 mmol L<sup>-1</sup> NaCl. A very strong change in the  $I_1/I_3$  ratio occurs close to 7 mmol L<sup>-1</sup> (CAC), indicating that pyrene migrates from the water ambient to the inner of the micelle (hydrophobic site) due to the formation of polymer–surfactant aggregation complex. It can also be seen that at concentrations higher than CAC, no plateau is formed; i.e., the  $I_1/I_3$  values keep decreasing with increase of surfactant concentration meaning that the micelles are still draining water. This fact indicates that the aggregates MC–DTAB formed in the presence of salt are loose, not very dense objects. The difference between the CAC values obtained from electrical conductivity and fluorescence is due to the presence of NaCl. It is well-known that the increase in the ionic strength of the medium decreases the parameters of aggregation such as CMC and CAC.



**Figure 3.** Frequency distribution of methylcellulose at different DTAB concentration at 25 °C. (—) without salt; (—○—) with NaCl.

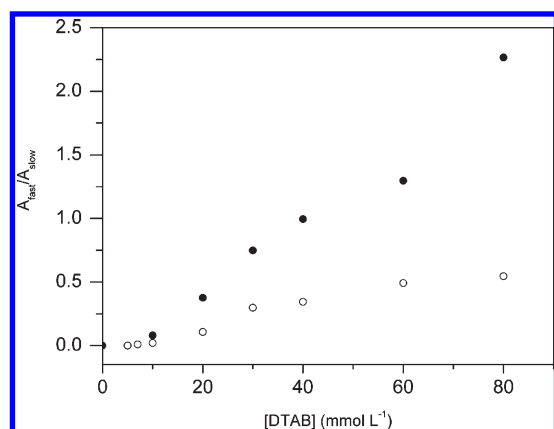
Figure 3 shows relaxation frequency distributions for the system MC–DTAB with 100 mmol L<sup>−1</sup> NaCl and without salt. For both systems, in the absence of surfactant, the time correlation function shows only one relaxation mode that may be assigned to single polymer chains. When the surfactant concentration was in the vicinity of the CAC or higher than it, two modes were detected. The slow mode corresponds to the MC–DTAB complex and the fast mode to the free micelles of DTAB as it can be concluded from the values of the respective hydrodynamic radii calculated by the Stokes–Einstein relation, shown in Figure 4. MC has a semiflexible chain whose conformation allows a contact between the methoxyl group of the polymer and the first carbon atoms of alkyl chain surfactant micelle diminishing the extension of these exposed hydrophobic areas with the water. A maximum in  $R_{h,slow}$ , in the absence of salt, occurs near 9 mmol L<sup>−1</sup> followed by a decrease and a subsequent linear increase. Otherwise, the system in the presence of salt shows only a linear increase of  $R_{h,slow}$ . For other polymer–surfactant systems, maxima either on viscosity or on the hydrodynamic radius were earlier reported.<sup>29,53,54</sup> In the present study, the maximum in  $R_{h,slow}$  in the absence of salt, occurs close to CAC determined through electrical conductivity. Furthermore, the increase of  $R_{h,slow}$  is not very pronounced in comparison to the free polymer thus we believe that the maximum is not due to interchain complexes but rather to expansion of the MC due to binding of surfactant micelles to the polymer, enhanced by the electrostatic repulsion between charged DTAB micelles along the polymer chain. Otherwise, for the system PEO–hexadecyltrimethylammonium chloride the maximum in radius of gyration and hydrodynamic radius was attributed to both reasons mentioned.<sup>55</sup> Moreover, for the system studied here beyond this maximum binding point, the slight decrease of  $R_{h,slow}$  may be attributed to electrostatic screening of the charge interactions by excess of counterions.<sup>56</sup> We can see also in



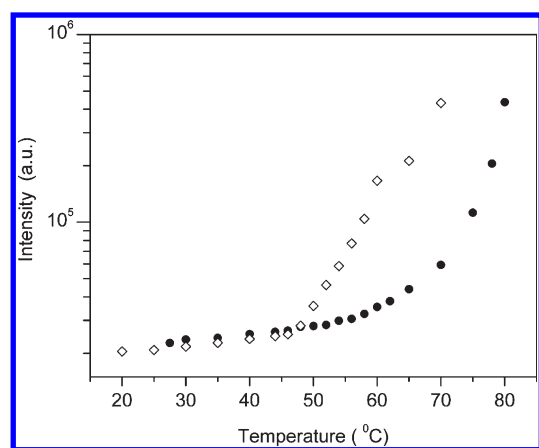
**Figure 4.** Apparent hydrodynamic radius as a function of surfactant concentration for the slow mode ( $R_{h,slow}$ ), (□) without salt and (♦) in presence of NaCl, and for the fast mode ( $R_{h,fast}$ ), (○) without salt and (●) in presence of NaCl.

Figure 4 that  $R_{h,fast}$  is approximately constant with increasing DTAB concentration and in the presence of NaCl the  $R_{h,fast}$  is higher than in absence of salt probably due to the electrostatic stabilization of shell leading to an increase in the size of the micelles with the increase in the ionic strength of the medium.

In Figure 5 the ratio of the amplitudes of fast to slow mode ( $A_{fast}/A_{slow}$ ) is plotted as a function of DTAB concentration. In the absence of salt, the slow mode predominates over the fast one because the values of  $A_{fast}/A_{slow}$  are lower than the unity. When



**Figure 5.** Amplitude ratio between the fast and slow mode for methylcellulose solution in different DTAB concentrations: (○) without salt; (●) in presence of NaCl.



**Figure 6.** Temperature variation of the intensity of scattered light at  $\theta = 90^\circ$  for aqueous solution of  $5 \text{ g L}^{-1}$  methylcellulose: (◇) without surfactant; (●) in presence of  $40 \text{ mmol L}^{-1}$  DTAB.

salt is added, the behavior of the amplitudes changes considerably. The slow mode predominates only up to  $40 \text{ mmol L}^{-1}$  DTAB. At higher surfactant concentrations, the free micelles become the main contributing mode reaching high values for the ratio  $A_{\text{fast}}/A_{\text{slow}}$ .

### B. Phase Separation and Sol–Gel Transition of MC–DTAB.

An aqueous MC solution is able to gel upon heating and gelation temperature is around  $62^\circ\text{C}$  for MC solution at  $5 \text{ g L}^{-1}$ .<sup>14,35,57</sup> Most additives can shift the sol–gel transition to higher or lower temperature from a pure MC solution.<sup>58,59</sup> It is very well-known that electrolytes such as NaCl can depress the gel temperature of aqueous MC solutions by salting out effect.<sup>60</sup> Here, the effect of DTAB on phase separation and sol–gel transition of MC was studied through SLS, rheology and micro DSC. For SLS measurements the used surfactant concentration was  $40 \text{ mmol L}^{-1}$ , which is well above the CAC. Figure 6 shows the dependence of the scattered intensity with the temperature at a scattering angle of  $90^\circ$  for aqueous MC and MC–DTAB solution at polymer concentration of  $5 \text{ g L}^{-1}$ . As can be seen MC solution presented a great increase of light scattering around  $50^\circ\text{C}$  that is attributed to the formation of large aggregates in solution due to phase separation. At phase separation temperature, it is observed an 21-fold increase

in the scattered light intensity. Previous works have shown that water-soluble cellulose derivatives, such as HPMC and MC, are good model systems for investigating the interference of phase separation and gelation, and that these are due to the hydrophobic interactions.<sup>61,62</sup> Shiomi et al.<sup>62</sup> suggested that phase separation and gelation in aqueous MC solutions are strongly coupled, and that phase separation occurs before the gel formation. The authors proposed a model to understand the relationship between phase separation and network formation. Briefly, the aqueous MC solution is transparent and homogeneous at room temperature. When the sample reaches a certain temperature, cross-linking points begin to form due to hydrophobic interactions. The increase in the apparent molecular weight by cross-linking induces the phase separation, resulting in a MC-rich phase and MC-poor phase. After the phase separation progresses to some extent, the MC-rich phase begins to gel, resulting in the gelation of entire system. Villetti et al.<sup>63</sup> showed that phase separation in aqueous MC solution in the presence of salt occurs by spinodal decomposition mechanism through small angle light scattering (SALS). Figure 6 shows also that MC–DTAB system presents an increase of light scattering at higher temperature,  $60^\circ\text{C}$ , due to the binding of the cationic surfactant on polymer chains. Above CAC the DTAB binds to MC chains, through hydrophobic interaction, resulting in a salting in effect. This phenomenon shifts the phase separation of MC to higher temperature.

In order to investigate the effect of DTAB on the gelation of MC dynamic viscoelastic measurements were performed for aqueous MC solutions at  $5 \text{ g L}^{-1}$  in the presence of different surfactant concentrations. Dynamic storage modulus  $G'$  and loss modulus  $G''$  as a function of temperature are shown in Figure 7, parts a and b, respectively. Several features can be observed from these results: (1) For pure MC solution,  $G'$  and  $G''$  increase linearly with temperature until  $62.5^\circ\text{C}$  at which a rapid increase in  $G'$  and  $G''$  is observed. (2) For pure MC solution,  $G'$  and  $G''$  reach the gel plateau at high temperature and the high  $G'$  ( $G' > 100 \text{ Pa}$ ) values compared to that  $G''$  ( $G'' < 10 \text{ Pa}$ ) indicates the formation of gel networks. (3) For MC–DTAB solutions,  $G'$  and  $G''$  in the gel plateau are lower than in the pure MC solution, meaning that the presence of DTAB decreases the gel strength. (4) The onset of the abrupt increase in both  $G'$  and  $G''$  shifts to lower temperature when surfactant concentration is lower or equal the CMC as compared to pure MC solution. Above the characteristic CMC of DTAB, the onset of the gelation process curve shifts to higher temperatures. Generally, the crossover of  $G'$  and  $G''$  is usually taken as the gelation temperature. However, some authors on the basis of rheological measurements suggested that the sharp increase in  $G'$  should be taken as the gel temperature.<sup>44</sup> Here, the latter criterion was used to determine the gelation temperature and these results are shown in Table 2. We can see the gelation temperature decreases as a function of DTAB concentration up to the CMC, above which a linear increase up to the highest concentration measured was observed.

Micro-DSC curves during heating for aqueous MC solutions at  $5 \text{ g L}^{-1}$  as a function of DTAB concentration are shown in Figure 8a, and corresponding peak temperatures are summarized in Figure 8b. For comparison, heating and cooling curves for MC at  $5 \text{ g L}^{-1}$  in the presence of  $5 \text{ mmol L}^{-1}$  DTAB are shown in Figure 8c. Several features can be identified upon heating: (1) in the absence of DTAB there is a single endothermic peak for pure MC; (2) DTAB affects the pattern of the sol–gel transition for MC. In the presence of  $5 \text{ mmol L}^{-1}$  DTAB (concentration lower than CMC) there is an endothermic main peak followed by a

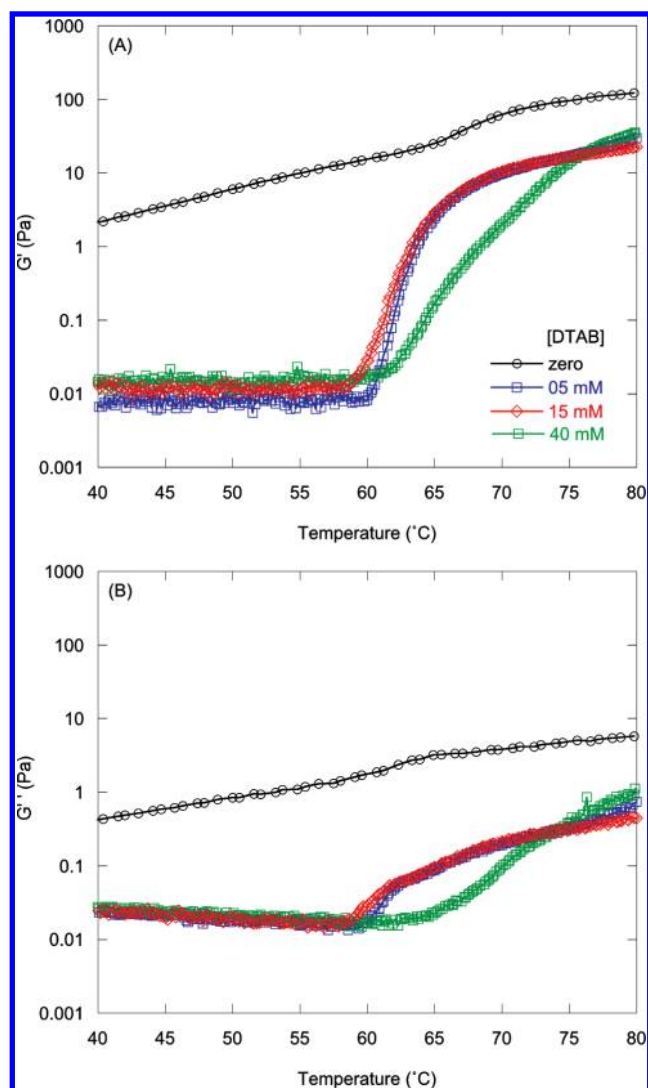


**Figure 7.** Dynamic storage modulus  $G'$  (a) and loss modulus  $G''$  (b) as a function of temperature for  $5.0 \text{ g L}^{-1}$  MC solutions in presence of different DTAB concentrations, as indicated.

**Table 2.** Gelation Temperature for MC in the Absence and Presence of DTAB

CTAB ( $\text{mmol L}^{-1}$ )	$T$ ( $^{\circ}\text{C}$ )
0	62.1
5	60.4
15	59.2
25	60.9
40	62.1

shoulder located at higher temperature. For DTAB concentrations higher than  $15 \text{ mmol L}^{-1}$  (CMC), a second shoulder at lower temperature is also observed; at  $40 \text{ mmol L}^{-1}$  DTAB concentration we can see the appearance of a bimodal endothermic peak suggesting that gelation occurs by two-step process at high surfactant concentration; (iii) DTAB shows transition from the salt-out to the salt-in effect close to CMC value during the gelation; the main endothermic peak shifts to the lower temperature for surfactant concentration lower than CMC, whereas

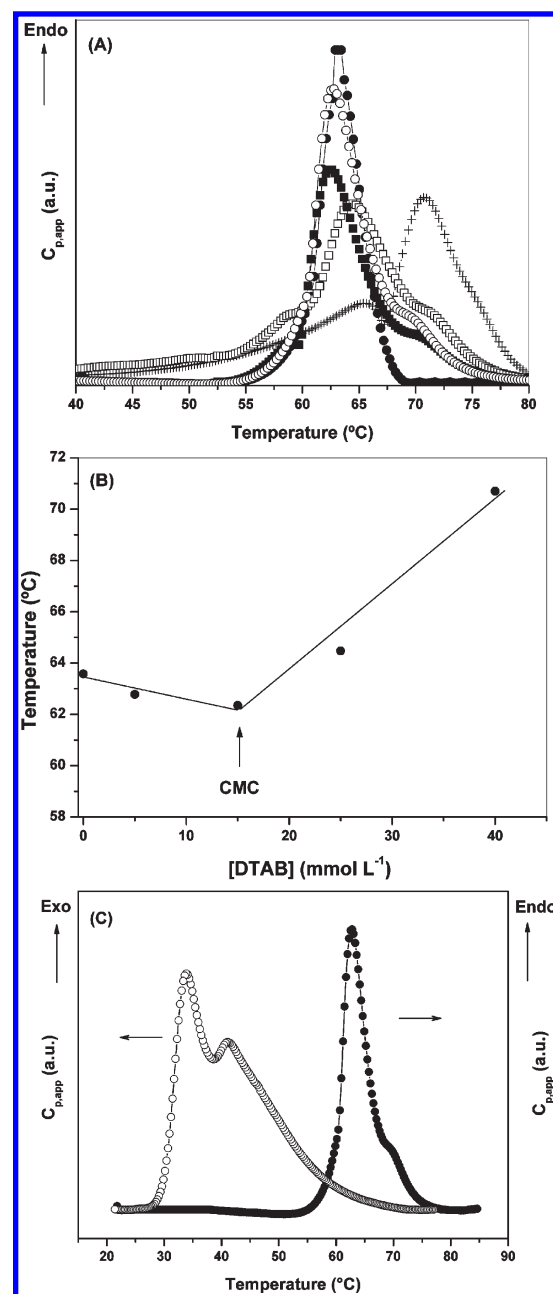


**Figure 8.** (a) Apparent thermal capacity  $C_{p,app}$  as a function of temperature for MC at  $5 \text{ g L}^{-1}$  in presence of different DTAB concentrations upon heating at  $1 \text{ }^{\circ}\text{C min}^{-1}$ : (—●—)  $0 \text{ mM}$ ; (—○—)  $5 \text{ mM}$ ; (—■—)  $15 \text{ mM}$ ; (—□—)  $25 \text{ mM}$ ; (—+-)  $40 \text{ mM}$ . (b) Peak temperature as a function of DTAB concentration obtained from micro-DSC measurements. (c) Apparent thermal capacity  $C_{p,app}$  as a function of temperature for MC at  $5 \text{ g L}^{-1}$  in presence of  $5 \text{ mmol L}^{-1}$  of DTAB concentration upon (—○—) heating and (—●—) cooling at  $1 \text{ }^{\circ}\text{C min}^{-1}$ .

the opposite is observed for DTAB concentrations higher than CMC. These results are in line with the rheological measurements.

The salt-out effect may be attributed to competition between bromide ions from DTAB and MC chains for water molecules. Therefore, hydrophobic interactions between MC chains are favored upon heating because water molecules available for MC chains decrease, leading to formation of a gel at a lower temperature in the presence of surfactant. This effect is similar



to the addition of NaCl to MC solutions. Otherwise, the salt-in effect may be interpreted considering that DTAB binds to MC through hydrophobic interactions forming a surfactant cage on MC chains. Therefore, a higher temperature is required to weaken the surfactant cages, so as to expose hydrophobic groups on MC to water and promote association to form a gel. From these results we can compare the effect of CTAB and DTAB on the gel formation process of MC. Li et al.<sup>35</sup> recently reported a single endothermic peak for the gelation of MC in the presence of CTAB surfactant by micro-DSC measurements. However, in the present study a bimodal endothermic peak was evidenced at high DTAB concentration.

This behavior can be explained by different binding strengths of each surfactant to MC. Since the alkyl chain is longer for CTAB than DTAB the hydrophobic part of the former associates more strongly with hydrophobic units on MC. Indeed, the CAC<sup>36</sup> of CTAB (0.42 mmol L<sup>-1</sup>) is 22-fold lower than DTAB (8.5 mmol L<sup>-1</sup>), thus indicating that DTAB is a weaker surfactant than CTAB because the latter can form hydrophobic interactions at a lower concentration. As MC–CTAB interactions are strong, we may suppose that most of the surfactant molecules are bound to polymer and form the surfactant cage on MC. Therefore, heating can disturb the MC–CTAB interaction and consequently allow the hydrophobic association of MC chains, resulting in a single endothermic peak. Likewise, it is reasonable to consider that the number of DTAB molecules that bind to MC is much less than that of CTAB. Accordingly, a number of MC chains are not bound to DTAB, and these free MC chains may associate first upon heating, leading to the first endothermic peak. The second peak is then evidenced at higher temperature when the surfactant cages of MC are destroyed allowing them to associate hydrophobically.

It is also interesting to compare the effect of DTAB and anionic surfactant SDS on the gelation of MC solutions. Both surfactants have the same hydrophobic chain length, and CAC of SDS (6 mmol L<sup>-1</sup>) and DTAB (8.5 mmol L<sup>-1</sup>) are not hugely different as compared to CTAB and DTAB. Wang et al.<sup>34</sup> also observed a bimodal endothermic gelation of MC–SDS, i.e., two-step gelation process when SDS concentration was higher than the characteristic CAC. This similarity in behavior in the profile of the sol–gel transition of MC–DTAB and MC–SDS systems is attributed to the strength of binding between surfactants on MC. Moreover, two exothermic peaks were evident upon cooling in both MC and MC–DTAB solutions. The cooling curve for MC at 5 g L<sup>-1</sup> in the presence of 5 mmol L<sup>-1</sup> DTAB is shown in Figure 8c. The heat transfer associated with the first processes at lower temperature is greater than the other one, and this relation does not change as a function of the surfactant concentration. In all cases, the peak position is not affected by the DTAB concentration, suggesting that the surfactant does not change the mechanism of gel–sol transition.

## CONCLUSIONS

In this work, the interaction between MC and DTAB was examined using electrical conductivity, fluorescence, light scattering, rheology and micro differential scanning calorimetry techniques. The CAC values obtained by electrical conductivity and fluorescence indicate that the onset of aggregation occurs at a lower concentration than the characteristic CMC, and it was taken as an evidence of binding of the cationic surfactant to the neutral polymer. Furthermore, the lower value of  $\Delta G_m^\circ$  for the

MC–DTAB system as compared to DTAB in aqueous solution demonstrates that polymer–surfactant interactions are thermodynamically favored, and that MC polymer induces the aggregation process.

Dynamic light scattering showed the conformation changes of MC polymer chains when the cationic surfactant is added. For the MC–DTAB system in the absence of salt, a maximum in hydrodynamic radius is observed with the increase of surfactant concentration. The maximum occurs due to the binding of DTAB micelles to MC, which is accompanied by a chain expansion. Beyond this maximum binding point the decrease of  $R_{h,slow}$  may be attributed to electrostatic screening of the charge interactions by excess of counterions in the solution. In contrast, the MC–DTAB system in the presence of salt shows only a linear increase of  $R_{h,slow}$ .

SLS, rheology, and micro-DSC results highlighted the effect of DTAB on phase separation and gelation of MC. Above the CMC the association MC–DTAB shifts the phase separation temperature to higher temperature when compared to pure MC. A good correlation between rheological and micro-DSC properties was observed. DTAB shows transition from salt-out to the salt-in effect on the gelation of MC at concentrations close to CMC. The cationic surfactant affects the pattern of the sol–gel transition as well as the gel strength. This behavior can be explained by taking into account the interaction strength polymer–surfactant. Surfactants with short alkyl chain associate more weakly with methoxyl group on MC than surfactants with high hydrophobicity.

## AUTHOR INFORMATION

### Corresponding Author

\*E-mail: mvilletti@smail.ufsm.br. Telephone: + 55 55 32208858. Fax: + 55 55 32208032.

## ACKNOWLEDGMENT

The authors acknowledge financial support from FAPERGS (Pronex 10/0005-1), CAPES (Edital pró-equipamentos no. 01/2007) and CNPq (no. 577442/2008-2). C.G. thanks the CNPq (Grant 558054/2009-9).

## REFERENCES

- (1) Lauten, R. A.; Nyström, B. *Colloids Surf., A* **2003**, 219, 45.
- (2) Holmberg, C.; Sundelof, L. O. *Langmuir* **1996**, 12, 883.
- (3) Kjoniksen, A. L.; Knudsen, K. D.; Nystrom, B. *Eur. Polym. J.* **2005**, 41, 1954.
- (4) Panmai, S.; Prud'homme, R. K.; Peiffer, D. G.; Jockusch, S.; Turro, N. J. *Langmuir* **2002**, 18, 3860.
- (5) Berglund, K. D.; Przybycien, T. M.; Tilton, R. D. *Langmuir* **2003**, 19, 2705.
- (6) Kjoniksen, A. L.; Knudsen, K. D.; Nystrom, B. *Eur. Polym. J.* **2005**, 41, 1954.
- (7) Edler, K. J.; Wasbrough, M. J.; Holdaway, J. A.; O'Driscoll, B. M. D. *Langmuir* **2009**, 25, 4047.
- (8) Bu, H.; Kjoniksen, A. L.; Elgsaeter, A.; Nyström, B. *Colloids Surf., A* **2006**, 278, 166.
- (9) Olsson, M.; Boström, G.; Karlson, L.; Piculell, L. *Langmuir* **2005**, 21, 2743.
- (10) Bai, D.; Khin, C. C.; Chen, S. B.; Tsai, C. C.; Chen, B. H. *J. Phys. Chem. B* **2005**, 109, 4909.
- (11) Dan, A.; Ghosh, S.; Moulik, S. P. *J. Phys. Chem. B* **2009**, 113, 8505.
- (12) Joshi, S. C.; Chen, B. *J. Appl. Polym. Sci.* **2009**, 113, 2887.
- (13) Florence, A. T.; Attwood, D. *Physicochemical Principles of Pharmacy*; MacMillan Press: London, 2003.

- (14) Sarkar, N. *J. Appl. Polym. Sci.* **1979**, *24*, 1073.
- (15) Li, L. *Macromolecules* **2002**, *35*, 5990.
- (16) Sovilj, V. J.; Petrovic, L. B. *Carbohydr. Polym.* **2006**, *64*, 41.
- (17) Su, J. C.; Liu, S. Q.; Joshi, S. C.; Lam, Y. C. *J. Appl. Polym. Sci.* **2008**, *93*, 495.
- (18) Bao, H.; Li, L.; Gan, L. H.; Zhang, H. *Macromolecules* **2008**, *41*, 9406.
- (19) Zanette, D.; Lima, C. F.; Ruzza, A. A.; Belarmino, A. T. N.; Santos, S. F.; Frescura, V. L. A.; Marconi, D. M. O.; Froehner, S. J. *Colloids Surf., A* **1999**, *147*, 89.
- (20) Hormnirun, P.; Sirivat, A.; Jamieson, A. M. *Polymer* **2000**, *41*, 2127–2132.
- (21) Wang, S. C.; Wei, S. C.; Chen, W. B.; Tsao, H. K. *J. Chem. Phys.* **2004**, *120*, 4980.
- (22) Muzzalupo, R.; Infante, M. R.; Pérez, L.; Pinazo, A.; Marques, E. F.; Antonelli, M. L.; Strinati, C.; La Mesa, C. *Langmuir* **2007**, *23*, 5963.
- (23) Dal Bó, A.; Schweitzer, B.; Felipe, A. C.; Zanette, D.; Lindman, B. *Colloids Surf., A* **2005**, *256*, 171.
- (24) Bai, G.; Gonçalves, C.; Gama, F. M.; Bastos, M. *Thermochim. Acta* **2008**, *467*, 54.
- (25) Avranas, A.; Iliou, P. *J. Colloid Interface Sci.* **2003**, *258*, 102.
- (26) Zanette, D.; Soldi, V.; Romani, A. P.; Gehlen, M. H. *J. Colloid Interface Sci.* **2002**, *246*, 387.
- (27) Evertsson, H.; Nilsson, S. *Carbohydr. Polym.* **1999**, *40*, 293.
- (28) Martins, R. M.; da Silva, C. A.; Becker, C. M.; Samios, D.; Christoff, M.; Bica, C. I. D. *Colloid Polym. Sci.* **2006**, *284*, 1353.
- (29) Martins, R. M.; da Silva, C. A.; Becker, C. M.; Samios, D.; Christoff, M.; Bica, C. I. D. *J. Braz. Chem. Soc.* **2006**, *17*, 944.
- (30) Morimoto, H.; Hashidzume, A.; Morishima, Y. *Polymer* **2003**, *44*, 943.
- (31) Miranda, J. A.; Cacita, N.; Okano, L. T. *Colloids Surf., B* **2007**, *60*, 19.
- (32) Drummond, C. J.; Albers, S.; Furlong, D. N. *Colloids Surf.* **1992**, *62*, 75.
- (33) Zana, R.; Lang, J.; Lianos, P. *J. Phys. Chem.* **1985**, *89*, 41.
- (34) Wang, Q.; Li, L.; Liu, E.; Xu, Y.; Liu, J. *Polymer* **2006**, *47*, 1372.
- (35) Li, L.; Liu, E.; Lim, C. H. *J. Phys. Chem. B* **2007**, *111*, 6410.
- (36) Dar, A. A.; Garai, A.; Das, A. R.; Ghosh, S. J. *J. Phys. Chem. A* **2010**, *114*, 5083.
- (37) Wang, G.; Olofsson, G. *J. Phys. Chem.* **1995**, *99*, 5588.
- (38) Sardar, N.; Ali, M. S.; Kamil, M.; Kabir-ud-Din. *J. Chem. Eng. Data* **2010**, *55*, 4990.
- (39) Holmberg, C.; Nilsson, S.; Singh, S. K.; Sundelof, L. O. *J. Phys. Chem.* **1992**, *96*, 871.
- (40) Kalyanasundaram, K.; Thomas, J. K. *J. Am. Chem. Soc.* **1977**, *99*, 2039.
- (41) Sierget, A. J. *MIT Radiat. Lab. Rep.* **1943**, 465.
- (42) Provencher, S. W. *Comput. Phys. Commun.* **1982**, *27*, 213.
- (43) Provencher, S. W. *Comput. Phys. Commun.* **1982**, *27*, 229.
- (44) Li, L.; Shan, H.; Yue, C. Y.; Lam, Y. C.; Tam, K. C.; Hu, X. *Langmuir* **2002**, *18*, 7291.
- (45) Zana, R.; Benrraou, M.; Rueff, R. *Langmuir* **1991**, *7*, 1072.
- (46) Kastner, U.; Zana, R. *J. Colloid Interface Sci.* **1999**, *218*, 468.
- (47) Nagarajan, R. *Colloids Surf.* **1985**, *13*, 1.
- (48) Witte, F. M.; Engberts, K. B. F. N. *J. Colloid Surf.* **1989**, *38*, 417.
- (49) Zana, R.; Binana-Limbele, W.; Kamenka, N.; Lindman, B. *J. Phys. Chem.* **1992**, *96*, 5461.
- (50) Lee, J. N.; Moroi, Y. *J. Colloid Interface Sci.* **2004**, *273*, 645.
- (51) Ray, G. B.; Chakraborty, L.; Ghosh, S.; Moulik, S. P.; Palepu, R. *Langmuir* **2005**, *21*, 10958.
- (52) Maiti, K.; Chakraborty, I.; Bhattacharya, S. C.; Panda, A. K. *J. Phys. Chem. B* **2007**, *111*, 14175.
- (53) Winnik, F. M.; Regismond, S. T. A. *Colloid Surf. A* **1996**, *118*, 1.
- (54) Holmberg, B.; Jonsson, B.; Kronberg, B.; Lindman, B. In: *Surfactants and Polymers in Solution*, 2nd ed.; Wiley: Sussex, U.K., 2003.
- (55) Mya, K. Y.; Sirivat, A.; Jamieson, A. M. *Macromolecules* **2001**, *34*, 5260.
- (56) Chari, K.; Antalek, B.; Lin, M. Y.; Sinhá, S. K. *J. Chem. Phys.* **1994**, *100*, 5294.
- (57) Kundu, P. P.; Kundu, M. *Polymer* **2001**, *42*, 2015.
- (58) Xu, Y.; Wang, C.; Tam, K. C.; Li, L. *Langmuir* **2004**, *20*, 646.
- (59) Xu, Y.; Li, L.; Zheng, P.; Lam, Y. C.; Hu, X. *Langmuir* **2004**, *20*, 6134.
- (60) Xu, Y.; Li, L. *Polymer* **2005**, *46*, 7410.
- (61) Kita, R.; Kaku, T.; Kubota, K.; Dobashi, T. *Phys. Lett. A* **1999**, *259*, 302.
- (62) Takeshita, H.; Saito, K.; Miya, M.; Takenaka, K.; Shiomi, T. *J. Polym. Sci. B Polym. Phys.* **2010**, *48*, 168.
- (63) Villetti, M. A.; Soldi, V.; Rochas, C.; Borsali, R. *Macromol. Chem. Phys.* **2011** 10.1002/macp.201000697.